



## OPEN ACCESS

## EDITED BY

Jian Liu,  
Qingdao Institute of Marine  
Geology (QIMG), China

## REVIEWED BY

Maosheng Gao,  
Qingdao Institute of Marine  
Geology (QIMG), China  
Tianyuan Zheng,  
Ocean University of China, China

## \*CORRESPONDENCE

Guanghui Zhan,  
✉ zhagh2007@126.com

## SPECIALTY SECTION

This article was submitted to Quaternary  
Science, Geomorphology and  
Paleoenvironment,  
a section of the journal  
Frontiers in Earth Science

RECEIVED 06 December 2022

ACCEPTED 13 March 2023

PUBLISHED 31 March 2023

## CITATION

Zhan G, Li J, Wang H, Wen X and Gu H  
(2023), Origin and hydrochemical  
evolution of confined groundwater in  
Shanghai, China.  
*Front. Earth Sci.* 11:1117132.  
doi: 10.3389/feart.2023.1117132

## COPYRIGHT

© 2023 Zhan, Li, Wang, Wen and Gu. This  
is an open-access article distributed  
under the terms of the [Creative  
Commons Attribution License \(CC BY\)](#).  
The use, distribution or reproduction in  
other forums is permitted, provided the  
original author(s) and the copyright  
owner(s) are credited and that the original  
publication in this journal is cited, in  
accordance with accepted academic  
practice. No use, distribution or  
reproduction is permitted which does not  
comply with these terms.

# Origin and hydrochemical evolution of confined groundwater in Shanghai, China

Guanghui Zhan<sup>1,2\*</sup>, Jingzhu Li<sup>1,2</sup>, Hanmei Wang<sup>1,2</sup>, Xiaohua Wen<sup>1,2</sup>  
and Hua Gu<sup>1,2</sup>

<sup>1</sup>Shanghai Institute of Geological Survey, Shanghai, China, <sup>2</sup>Key Laboratory of Land Subsidence Monitoring and Prevention, MNR, Shanghai, China

Confined groundwater is an indispensable resource for the urban security of Shanghai, China, where multi-layer aquifer structures and human activities create a complex groundwater environment. An understanding of the hydrochemical characteristics and evolutionary mechanisms of groundwater is necessary for its protection and effective utilization and will be explored in this study. A total of 87 groundwater samples were collected from five confined aquifers. Hydrochemistry analysis methods such as Durov diagram, Gibbs model and Saturation index were used to determine the origin and hydrochemical evolution of the confined groundwater. The results show that the samples have two different origins, marine–continental and continental, which have different hydrochemical characteristics.  $\text{Cl}^-$  content of  $7.5 \text{ meq L}^{-1}$  was used as a demarcation index for the two origins. The groundwater with a marine–continental-origin is dominated by ancient seawater from which  $\text{Na}^+$  and  $\text{Cl}^-$  are derived, whereas  $\text{Ca}^{2+}$ ,  $\text{Mg}^{2+}$ , and  $\text{HCO}_3^-$  are derived mainly from carbonate dissolution. Groundwater with a continental-origin is dominated by the effects of water–rock interaction, where major ions are derived mainly from silicate weathering and carbonate dissolution. In both types of groundwater,  $\text{SO}_4^{2-}$  is mainly derived from insoluble sulfides that are present in low quantities, whereas  $\text{SO}_4^{2-}$  in the few samples with high insoluble sulfide content is derived from human activities. Cation exchange is another controlling factor regarding the hydrochemical composition of groundwater, and water from the two origins have different reaction modes as follows: reverse cation exchange is dominant in marine–continental groundwater, whereas positive cation exchange is more common in continental groundwater. Over the past century, saline water has been flowing into the groundwater funnel region due to human activities, which has resulted in changes in the hydrochemical composition. The recent influx of fresh groundwater and artificial recharge has caused groundwater salinization and mineral re-dissolution.

## KEYWORDS

hydrochemistry, groundwater origin, Shanghai, water–rock interaction, ion source

## 1 Introduction

Confined groundwater is an important high-quality water resource for domestic and industrial purposes (Zhang et al., 2016), but its over-use causes serious problems. Globally, changes in the hydrochemical composition of groundwater threatens resources in many regions, especially in economically developed delta areas (Gan et al., 2018; Wang et al., 2022).

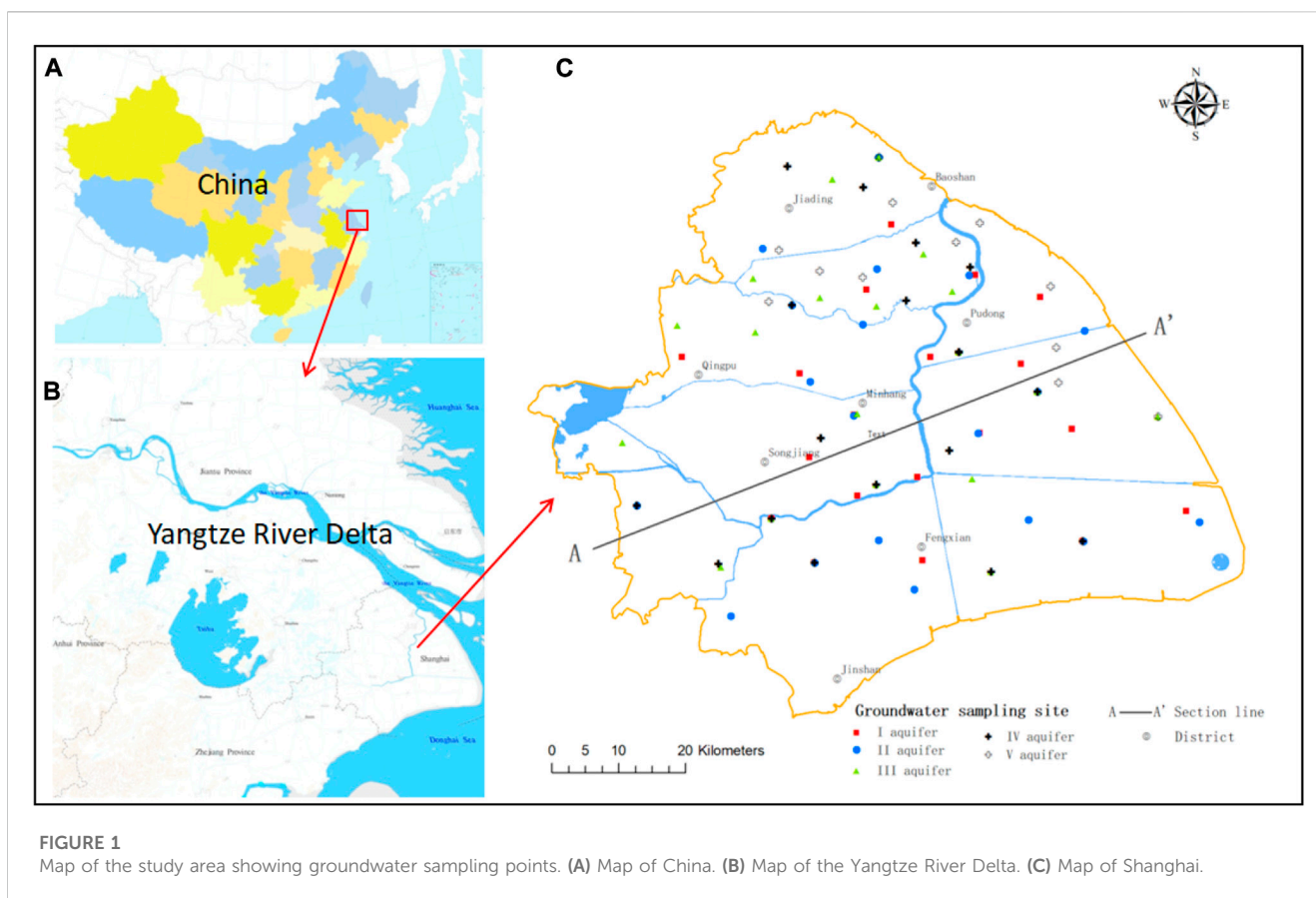


FIGURE 1

Map of the study area showing groundwater sampling points. (A) Map of China. (B) Map of the Yangtze River Delta. (C) Map of Shanghai.

Therefore, an understanding of the hydrochemical origins and controlling factors of groundwater is necessary for its development and protection.

The five confined aquifers in the Shanghai study area developed in an unconsolidated alluvial formation deposited under alternating marine and continental sedimentary environments. There is a weak hydraulic connection between the five aquifers, except where the aquifers are physically connected. Large quantities of high-quality groundwater are confined in Shanghai (Zhang et al., 1999), which has provided an enormous contribution to economic development over recent decades (Jang et al., 2012). However, over-exploitation and artificial recharge have greatly affected the groundwater environment, and its hydrochemical composition has considerably changed in some regions. Increasing attention had been focused on fluctuations in groundwater levels because of the serious land subsidence caused by groundwater exploitation (Huang et al., 2021; Li et al., 2021), but there have been few reports on the hydrochemical characteristics and evolutionary mechanisms of groundwater, and the use and protection of groundwater has received little attention. The origins of groundwater, hydrochemical characteristics, and its classification should be considered in detail to delineate groundwater boundaries and predict saline expansion/contraction (Yang et al., 2018; Li et al., 2022). The Yangtze River Delta is an ideal location to conduct such a study.

The aim of this study was to apply hydrochemical methods in (1) describing groundwater hydrochemical characteristics, 2)

identifying sources of groundwater and establishing their demarcation index, 3) identifying the sources of major ions in groundwater, 4) explaining the hydrochemical evolution of the water of different origins, and 5) elucidating the influence of human activities on groundwater. As a result, these methods provide a scientific basis for groundwater utilization and protection planning.

## 2 Materials and methods

### 2.1 Study area

The study area is the mainland part of Shanghai in the flat alluvial plain of the Yangtze River Delta at the mouth of the Changjiang River with an area of 5,300 km<sup>2</sup> within 120°52'–122°12'E and 30°40'–31°53'N (Figure 1). Quaternary deposits are widely distributed in the area with a thickness of 250–350 m increasing W–E. The aquifers are comprised mainly sand and clay in loose Quaternary sediments and include apfretic aquifers and five confined aquifers (Figure 2). This study focused on the latter.

Aquifers I–V were formed during the early to middle–late Pleistocene and their characteristics are shown in Table 1.

The groundwater system in the study area is not a stand-alone system and is part of the Yangtze River Delta system, where confined aquifers are the predominant type. In its natural state, groundwater



FIGURE 2 Cross-section showing hydrological conditions along the (A,A') transect.

TABLE 1 Characteristics of aquifers in the study area.

Aquifer	I	II	III	IV	V
Depositional age	Q <sub>3</sub> <sup>2</sup>	Q <sub>3</sub> <sup>1</sup>	Q <sub>2</sub> <sup>2</sup>	Q <sub>1</sub> <sup>1</sup>	Q <sub>1</sub> <sup>1</sup>
Depositional environment	Coastal-fluvial	Coastal-fluvial	Coastal-fluvial	Fluvial	Fluvial
Lithology	Fine sand	Medium sand	Medium sand and coarse sand	Medium sand, coarse sand	Medium sand and gravel
Depth (m)	30–40	60–70	110–120	130–180	250–280
Thickness (m)	3–18	20–30	20–30	60–80	10–40
Water yield of a single well (m <sup>3</sup> /d)	300–500	1,000–3000	1,000–3000	3000–5,000	1,000–3000

flows mainly NW–SE. In general, the groundwater is characterized by weak hydrodynamic conditions and a low flow rate. Recharge is mainly through lateral inflow, although artificial recharge has become an important source in recent decades, and discharge is mainly from anthropogenic extraction.

## 2.2 Sampling and analysis

For sampling, 87 wells were selected to provide a balanced regional distribution. Groundwater samples were collected in September 2018, and 19, 19, 19, 17, and 13 samples were collected from aquifers I–V, respectively (Figure 1).

Prior to filling, all sample bottles were rinsed three times with sample water. Samples for the cation analysis were collected in 500-mL HDPE bottles and then five drops of concentrated nitric acid were added; those for anion analysis were collected in 1000-mL glass bottles without preservatives. All samples were stored

on ice in the field and transferred to 4°C storage until ready for analysis.

The concentrations of Na<sup>+</sup>, K<sup>+</sup>, Ca<sup>2+</sup>, Mg<sup>2+</sup>, Cl<sup>-</sup>, and SO<sub>4</sub><sup>2-</sup> were determined by ion chromatography, HCO<sub>3</sub><sup>-</sup> was determined by acid–base titration, and total dissolved solid (TDS) concentrations were determined using gravimetric analysis (drying at 105 °C). The analysis accuracy was assessed through the ion-balance error of ±5%.

## 2.3 Durov diagram

The Durov diagram, which is used to study hydrochemical characteristics and facies (An et al., 2014; Gu et al., 2018), comprises two triangles, a central square, and two rectangles (Figure 5). The left and top triangles indicate the concentrations of cations and anions, respectively, the central square shows hydrochemical facies, and the right and bottom rectangles indicate TDS concentration and pH, respectively.

TABLE 2 Analysis results for confined groundwater samples.

Aquifer	Index	Unit	Min	Max	Mean	SD
I	pH	-	6.99	8.36	7.49	0.36
	K <sup>+</sup>	mg/l	1.61	38.25	12.18	11.50
	Na <sup>+</sup>	mg/l	154.64	2206.16	1,119.16	594.68
	Ca <sup>2+</sup>	mg/l	62.20	958.43	334.36	220.97
	Mg <sup>2+</sup>	mg/l	69.19	422.94	186.31	85.32
	HCO <sub>3</sub> <sup>-</sup>	mg/l	31.49	1,280.86	448.62	296.23
	CL <sup>-</sup>	mg/l	550.24	5,942.06	2644.55	1,376.07
	SO <sub>4</sub> <sup>2-</sup>	mg/l	0.20	13.53	4.23	4.06
	TDS	mg/l	1,306	9690	4562	2206
	II	pH	-	7.06	8.36	7.52
K <sup>+</sup>		mg/l	1.10	64.01	12.11	13.71
Na <sup>+</sup>		mg/l	35.12	2676.06	866.57	867.31
Ca <sup>2+</sup>		mg/l	35.28	584.68	240.95	155.66
Mg <sup>2+</sup>		mg/l	20.97	302.81	140.95	98.70
HCO <sub>3</sub> <sup>-</sup>		mg/l	15.74	648.77	294.55	153.86
CL <sup>-</sup>		mg/l	4.49	5,518.66	2031.00	1864.13
SO <sub>4</sub> <sup>2-</sup>		mg/l	0.67	28.58	6.56	6.84
TDS		mg/l	316	8846	3475	2869
III	pH	-	6.92	9.42	7.86	0.66
	K <sup>+</sup>	mg/l	1.21	81.03	12.97	20.06
	Na <sup>+</sup>	mg/l	32.10	4727.98	870.89	1,347.78
	Ca <sup>2+</sup>	mg/l	3.97	789.17	167.15	238.51
	Mg <sup>2+</sup>	mg/l	8.37	414.43	116.45	149.88
	HCO <sub>3</sub> <sup>-</sup>	mg/l	39.04	687.66	282.55	152.07
	CL <sup>-</sup>	mg/l	3.83	9310.29	1781.92	2773.69
	SO <sub>4</sub> <sup>2-</sup>	mg/l	0.20	1,131.02	64.26	258.43
	TDS	mg/l	250	16,522	3176	4648
IV	pH	-	7.30	9.38	8.04	0.56
	K <sup>+</sup>	mg/l	1.32	19.38	4.20	4.18
	Na <sup>+</sup>	mg/l	65.67	2007.69	298.84	456.31
	Ca <sup>2+</sup>	mg/l	4.22	262.67	54.01	68.98
	Mg <sup>2+</sup>	mg/l	9.81	263.52	44.02	59.83
	HCO <sub>3</sub> <sup>-</sup>	mg/l	21.97	416.88	252.28	129.67
	CL <sup>-</sup>	mg/l	6.32	4437.07	519.81	1,051.50
	SO <sub>4</sub> <sup>2-</sup>	mg/l	0.20	55.38	7.31	13.38
	TDS	mg/l	246	7010	1,084	1,593
V	pH	-	7.50	9.09	8.22	0.45
	K <sup>+</sup>	mg/l	1.83	18.79	5.59	4.58

(Continued in next column)

TABLE 2 (Continued) Analysis results for confined groundwater samples.

Aquifer	Index	Unit	Min	Max	Mean	SD
	Na <sup>+</sup>	mg/l	105.18	628.03	283.28	160.89
	Ca <sup>2+</sup>	mg/l	6.37	91.21	25.45	23.05
	Mg <sup>2+</sup>	mg/l	17.01	80.93	38.15	20.88
	HCO <sub>3</sub> <sup>-</sup>	mg/l	78.72	499.37	240.87	124.96
	CL <sup>-</sup>	mg/l	65.23	1,114.87	421.01	362.02
	SO <sub>4</sub> <sup>2-</sup>	mg/l	0.20	192.27	23.02	54.78
	TDS	mg/l	342	1974	940	526

## 2.4 Gibbs model

The Gibbs model is effective in elucidating hydrochemical processes (Gibbs, 1970; Gibbs, 1972). This model is based on groundwater hydrochemical processes being mainly controlled by water–rock interaction, evaporation, and precipitation (Farid et al., 2015; Wang et al., 2022). For this study area, the hydrochemical processes were adjusted to include rock–water interaction, marine-origin, and recharge (including lateral inflow and artificial recharge).

## 2.5 Saturation index

The saturation index (SI) is used to describe the solubility equilibrium of minerals in water (Rezaei et al., 2005).  $SI = \log(IPA/Ksp)$ , where IPA is the ionic activity product of dissolved mineral constituents and Ksp is the solubility product of the mineral. SI values of 0, >0, and <0 indicate saturated, supersaturated (precipitation may occur), and undersaturated (dissolution may occur) groundwater, respectively.

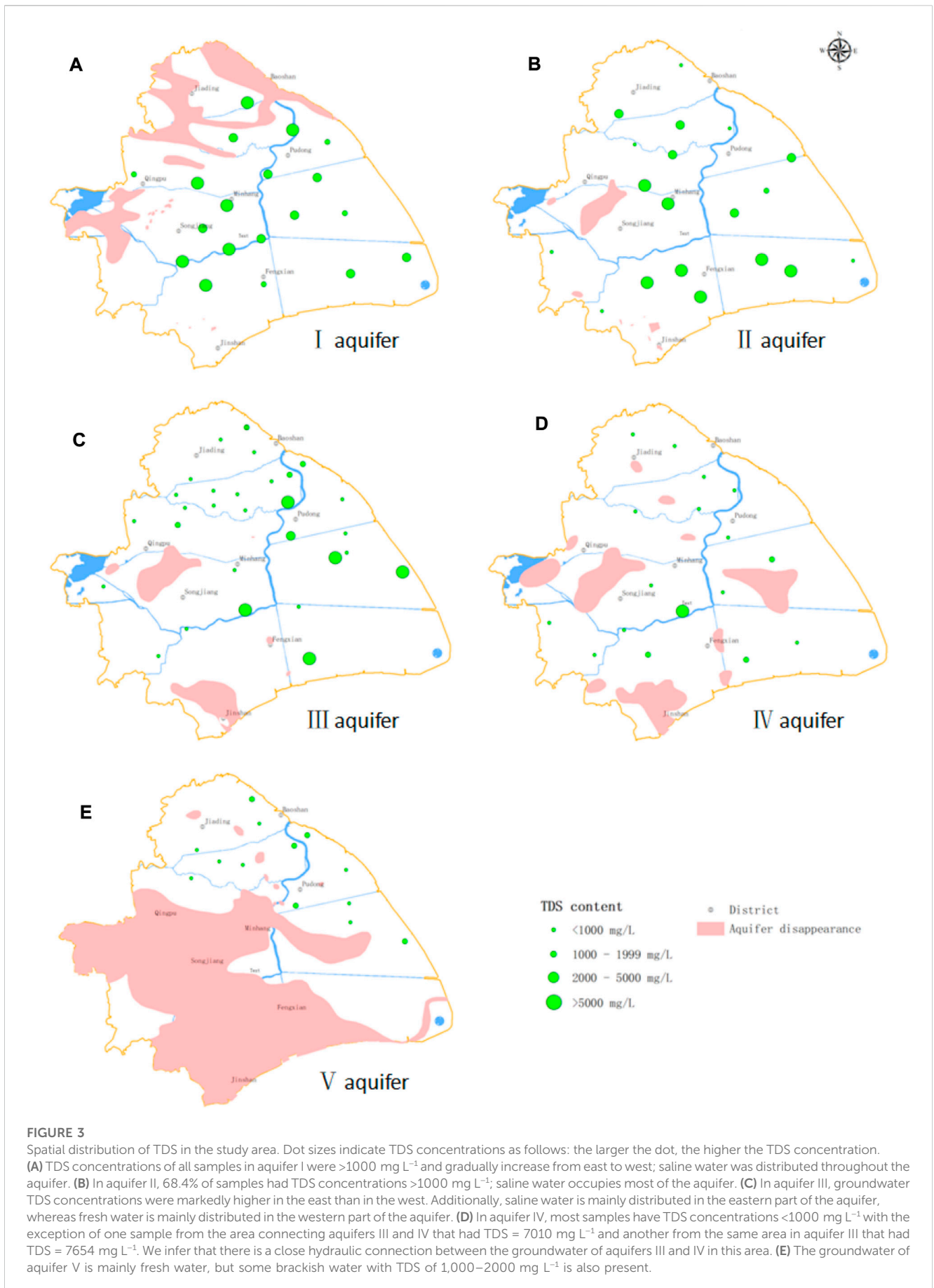
## 3 Results and discussion

### 3.1 Hydrochemical characteristics of confined groundwater

The ionic contents of the studied samples are shown in Table 2. The hydrochemical characteristics of aquifers I and II were generally similar, as were those of aquifers IV and V. The ion contents of aquifer III were the most variable with high standard deviation (SD) values, which indicated that the spatial distribution of groundwater is somewhat variable in terms of hydrochemical composition.

The pH values of groundwater were in the range of 6.99–8.36, 7.06–8.36, 6.92–9.42, 7.30–9.38, and 7.50–9.09 for aquifers I–V, respectively. Aquifers I–III were neutral to slightly alkaline, and aquifers IV–V were slightly alkaline with the pH increasing from aquifers I to V.

TDS concentrations had a range of 246–16522 mg L<sup>-1</sup> and decreased from aquifers I to V (Figure 3). All groundwater samples in aquifer I were saline water with TDS >5000 mg L<sup>-1</sup> in the west. In aquifer II, 68.4% of the samples were saline, with most in the southwest



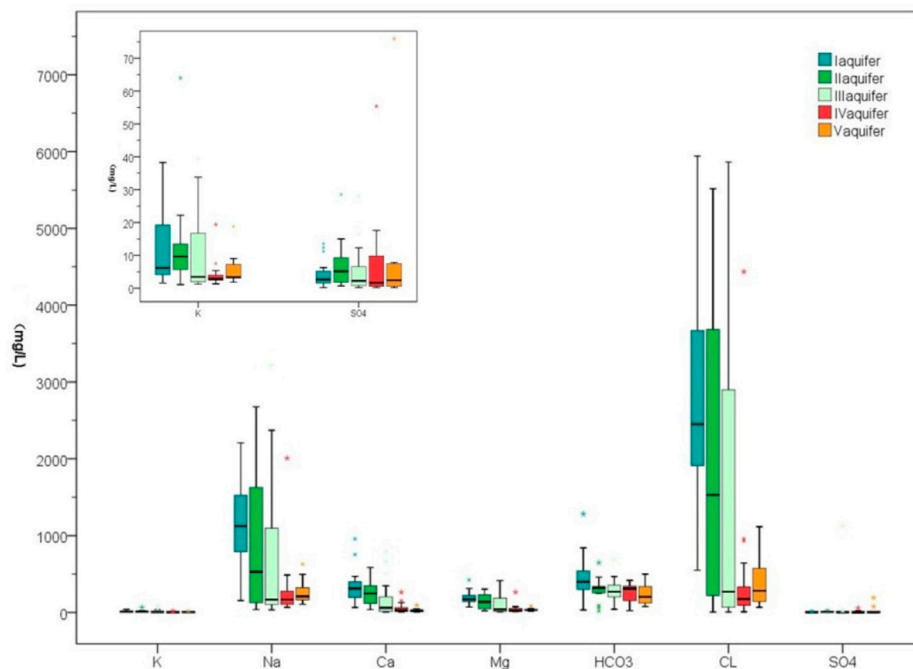


**FIGURE 4**  
Ranges of major-ion concentrations in confined groundwater aquifers.

having TDS  $>5000$  mg  $L^{-1}$ . There was a wide range of TDS concentrations in aquifer III, from 250 to 16522 mg  $L^{-1}$ , with fresh water predominating in the west and saline water in the east. In aquifers IV and V, most samples were fresh water. There were a few samples with TDS  $>2000$  mg  $L^{-1}$  in the area connecting aquifers III and IV.

The range of concentrations of the major ions are shown in [Figure 4](#).  $Na^+$  was the dominant cation with an order of  $Na^+ > Ca^{2+} > Mg^{2+} > K^+$ . Of the anions,  $Cl^-$  had the highest concentrations with clear dominance among all major ions in aquifers I–III. The concentrations of  $K^+$ ,  $Na^+$ ,  $Ca^{2+}$ ,  $Mg^{2+}$ , and  $Cl^-$  generally decreased from aquifers I to III but had similar concentrations in aquifers IV and V. Most samples had low  $SO_4^{2-}$  and  $HCO_3^-$  concentrations from all five aquifers ([Table 2](#)).

### 3.2 Hydrochemical facies of confined groundwater

The hydrochemical compositions and characteristics of the groundwater samples are indicated by the Durov diagram ([Figure 5](#)), where samples from aquifers I and II are concentrated on the  $Na^+$  and  $Cl^-$  sides and those from aquifers III–V are scattered in the upper half of the central square. This indicates that the predominant hydrochemical facies of aquifers I and II are Cl–Na, whereas those of aquifers III–V are variable.

The hydrochemical facies of groundwater can also be described in terms of TDS as follows: for TDS of  $<1000$  mg  $L^{-1}$ , hydrochemical facies were variable and included  $HCO_3^-Cl-Na$ ,  $Cl-HCO_3^-Na$ ,  $HCO_3^-Cl-Na-Mg$ , and  $Cl-HCO_3^-Na-Mg$ , which were mainly distributed in aquifers II–V. For a TDS of 1,000–2000 mg  $L^{-1}$ , the

hydrochemical facies were Cl–Na, Cl–Na–Ca, and Cl–Na–Mg, and these are distributed mainly in aquifers I, IV, and V. For TDS of 2000–5000 mg  $L^{-1}$ , the hydrochemical facies were Cl–Na–Ca and Cl–Na, which were mainly distributed in aquifers I and II. For TDS  $>5000$  mg  $L^{-1}$ , the hydrochemical facies were Cl–Na and distributed mainly in aquifers I–III.

### 3.3 Hydrochemical processes in confined groundwater

The Gibbs diagrams for all groundwater samples are shown in [Figure 6](#). Most samples from aquifers I and II are plotted in the marine-origin domain, whereas those from aquifer III are plotted in both the marine-origin and rock–water-interaction domains, and those from aquifers IV and V are plotted in the rock–water-interaction domain. However, some samples from aquifers IV and V deviate from the Gibbs model ([Figure 6A](#)). Therefore, we speculate that other factors may affect the composition of groundwater, which makes  $Na^+$  rich and  $Ca^{2+}$  poor. A similar pattern of evolution applies to aquifers I–III as discussed in the following section.

Quaternary strata studies ([Qiu and Li, 2007](#)) indicate that there were seven marine transgressions in Shanghai during the Quaternary period with aquifers I–III formed during transgression periods. The presence of groundwater of marine–continental- and continental-origin in the study area was verified. The distribution of the former may account for most of aquifers I and II, and the eastern portion of aquifer III. The latter applies to the remaining aquifers, including small portions of aquifers II and III and most of aquifers IV and V. Further evidence is provided in the following section based on an ion-ratio analysis.

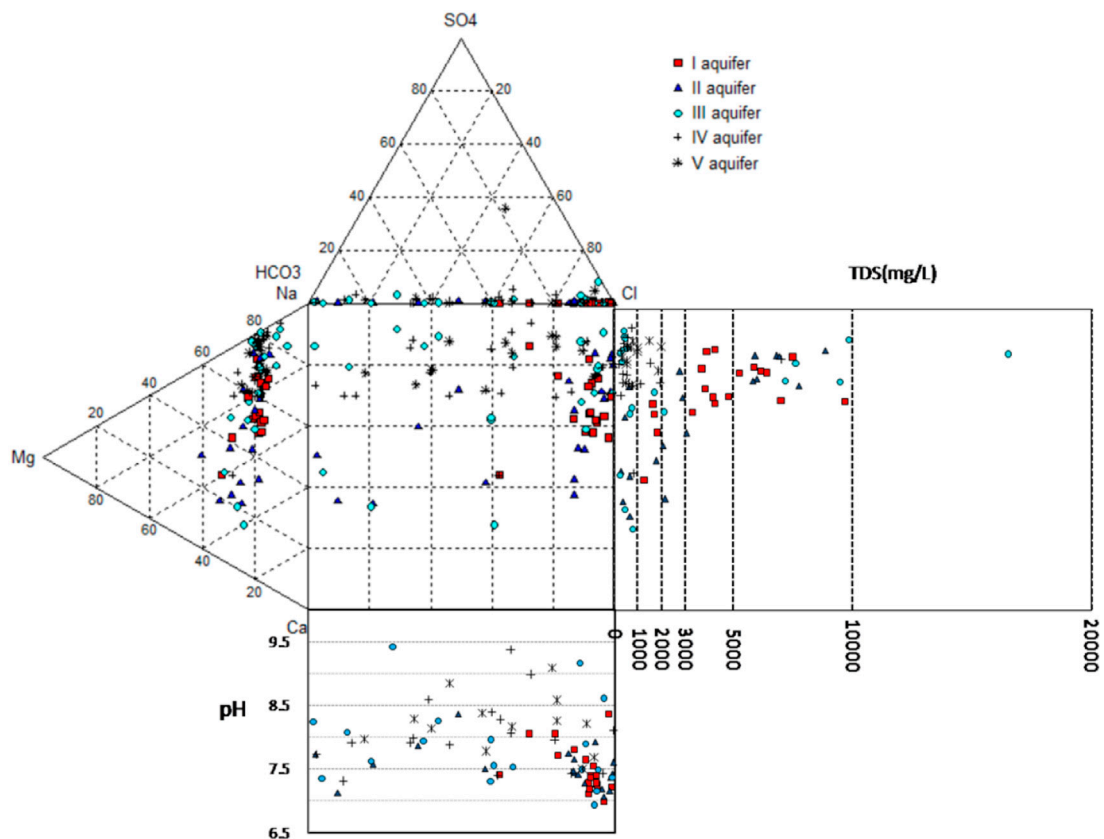


**FIGURE 5**  
Durov diagram for confined groundwater samples.

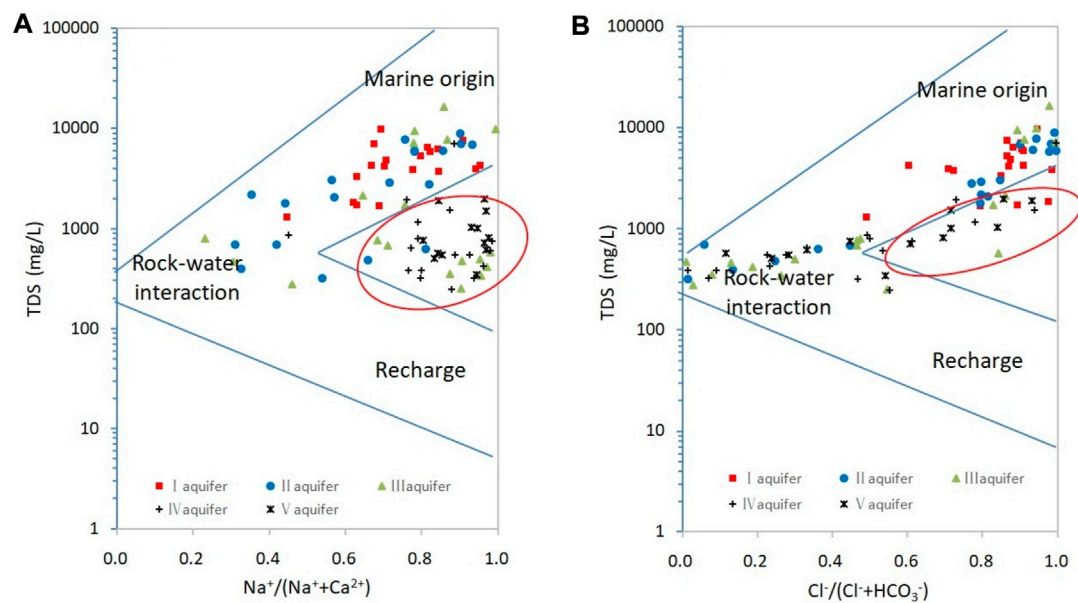
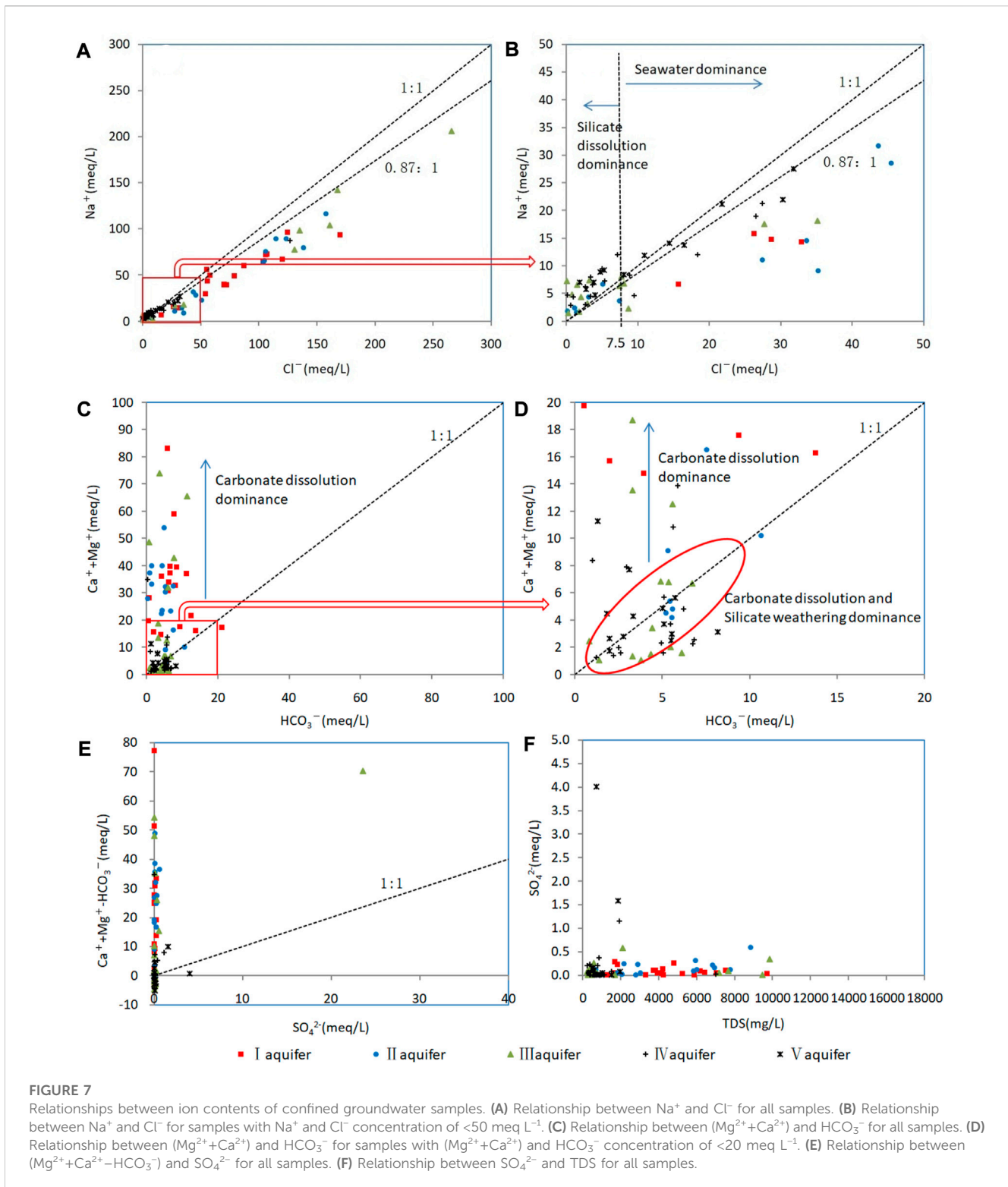


**FIGURE 6**  
Gibbs diagrams for confined groundwater. The red circles indicate samples that deviate from the Gibbs model. (A) Gibbs diagrams of ions. (B) Gibbs diagrams of anions.



### 3.4 Sources of ions in confined groundwater

The Quaternary sediments in the study area are comprised sand and clay. X-ray diffraction and electron microscopy data for these sediments (Qiu and Li, 2007) indicate that the diagenetic minerals

in the aquifers are predominantly silicate (quartz, feldspar, kaolinite, and illite) and carbonate (calcite and dolomite) rocks. Rock weathering and dissolution are naturally controlled by the hydrochemical composition of groundwater (Bau et al., 2004; Kim, 2010) through typical reactions as follows:

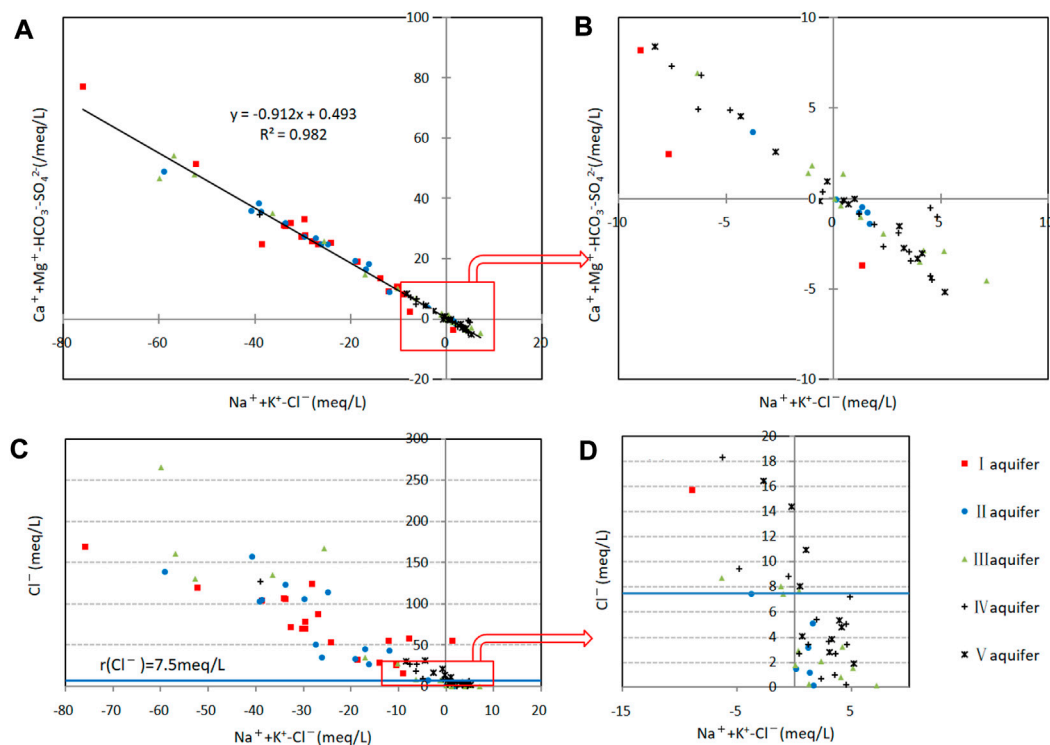
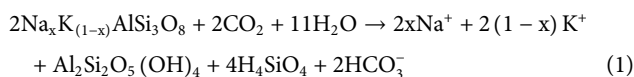


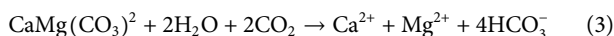
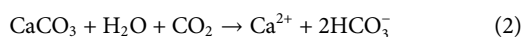
FIGURE 8

Cation-exchange analysis diagram of confined groundwater. (A) Relationship between  $(\text{Mg}^{2+} + \text{Ca}^{2+} - \text{HCO}_3^- - \text{SO}_4^{2-})$  and  $(\text{Na}^+ + \text{K}^+ - \text{Cl}^-)$  for all samples. (B) Relationship between  $(\text{Mg}^{2+} + \text{Ca}^{2+} - \text{HCO}_3^- - \text{SO}_4^{2-})$  and  $(\text{Na}^+ + \text{K}^+ - \text{Cl}^-)$  for samples with low concentrations. (C) Relationship between  $\text{Cl}^-$  and  $(\text{Na}^+ + \text{K}^+ - \text{Cl}^-)$  for all samples. (D) Relationship between  $\text{Cl}^-$  and  $(\text{Na}^+ + \text{K}^+ - \text{Cl}^-)$  for samples with low concentrations.

Silicate dissolution:



Carbonate dissolution:



Halite dissolution:



Ancient seawater is an important source of  $\text{Na}^+$  and  $\text{Cl}^-$  in the groundwater of marine-continental-origin. The  $\text{Na}^+/\text{Cl}^-$  equivalence ratio in seawater is 0.87 (Kunwar and Kawamura, 2014). A ratio of  $<1$  indicates that the groundwater is affected mainly by seawater, whereas ratios of  $>1$  indicate that silicate dissolution is more important (Eq. 1) and a ratio of 1 indicates that halite dissolution is the primary source of these ions (Eqs 4, 5; Gianguzza et al., 2004; Panno et al., 2006).

Bivariate plots for  $\text{Na}^+$  and  $\text{Cl}^-$  are shown in Figures 7A–B, which shows two groups of samples separated by the  $\text{Cl}^- = 7.5 \text{ meq L}^{-1}$  line (Figure 7B). Samples from aquifers I and II are distributed mainly below the 0.87:1 line with  $\text{Cl}^- > 7.5 \text{ meq L}^{-1}$ , and samples from aquifers IV and V are distributed mainly above the 1:1 line with  $\text{Cl}^- < 7.5 \text{ meq L}^{-1}$ .

Therefore, the  $\text{Cl}^- = 7.5 \text{ meq L}^{-1}$  line acts as a demarcation index to identify groundwater origins in the study area. Some samples from the aquifer V plot near the 1:1 line with  $\text{Cl}^- > 7.5 \text{ meq L}^{-1}$  is due to halite dissolution rather than seawater. Using the demarcation index of  $\text{Cl}^- = 7.5 \text{ meq L}^{-1}$ , it was determined that the proportions of continental-origin groundwater samples in aquifers I–V were 0%, 26.3%, 52.6%, 70.6%, and 84.6%, respectively.

Carbonate dissolution and silicate weathering are the primary sources of  $\text{Ca}^{2+}$ ,  $\text{Mg}^{2+}$ , and  $\text{HCO}_3^-$  as indicated by the  $(\text{Mg}^{2+} + \text{Ca}^{2+})/\text{HCO}_3^-$  ratio (Kenoyer and Bowser, 1992; Kim, 2010): a ratio of  $<1$  indicates that  $\text{Ca}^{2+}$  and  $\text{Mg}^{2+}$  were derived primarily from silicate weathering, and ratios of  $\leq 1$  indicate they were derived primarily from carbonate dissolution.

Most samples from aquifers I and II and the east part of aquifer III have  $(\text{Mg}^{2+} + \text{Ca}^{2+})/\text{HCO}_3^-$  ratios of  $>1$  (Figure 7C), which suggests carbonate dissolution as a source of  $\text{Ca}^{2+}$  and  $\text{Mg}^{2+}$ . Most samples from aquifers IV and V and the west part of aquifer III have ratios of  $\leq 1$ , which reflects the predominant contributions of silicate weathering and carbonate dissolution. Calcite and dolomite reach saturation or oversaturation in most samples ( $\text{SI} > -0.5$ ; Figures 10C, D), which indicates that carbonate dissolution occurred throughout geological history. In summary, carbonate dissolution made the greatest contribution to marine-continental-origin groundwater, whereas both silicate weathering and carbonate dissolution contributed to continental-origin groundwater.

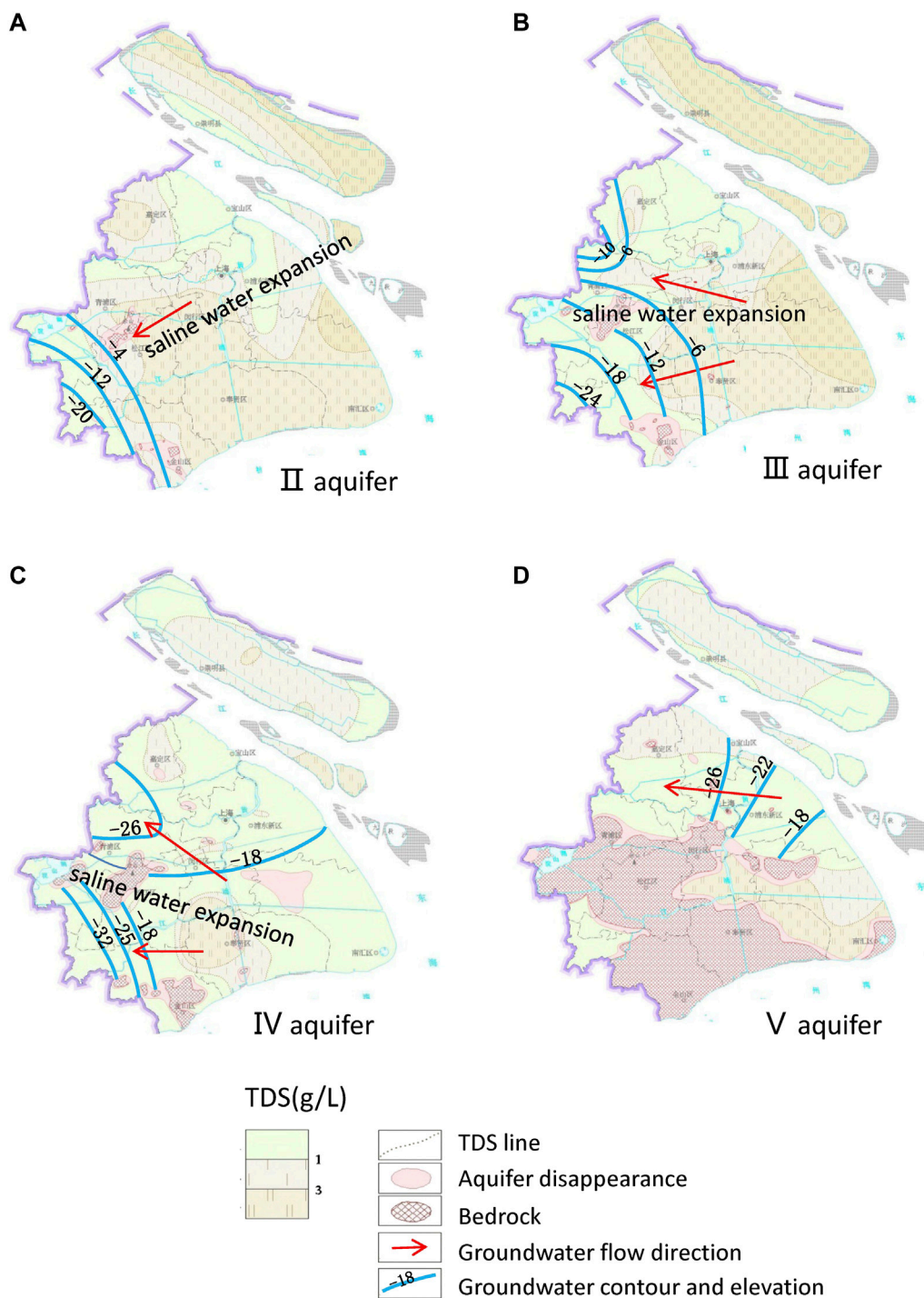
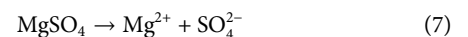
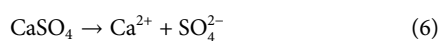


**FIGURE 9**

TDS and groundwater levels in the study area in 2009. TDS data are derived from [Wei et al. \(2010\)](#). Groundwater levels and flow directions are derived from [Gong, \(2009\)](#). (A) Groundwater funnels in aquifer II were mainly located in Songjiang in the southwest of the study area. (B) Groundwater funnels in aquifer III were mainly located in Songjiang and Qindu in the western part of the study area. (C) Groundwater funnels in aquifer IV are similar to those in aquifer III. Saline recharge from aquifer III to aquifer IV in the area connecting the aquifers has been exacerbated by a decline in groundwater levels in aquifer IV. (D) Groundwater generally flowed from east to west due to the decline in groundwater levels in the west part of aquifer V.

In the absence of anthropogenic sources,  $\text{SO}_4^{2-}$  is derived mainly from evaporite deposits, such as gypsum, through hydrochemical reactions as follows:



The  $\text{SO}_4^{2-}$  content of most samples was low ([Figure 7F](#)), and the correlations between  $(\text{Mg}^{2+} + \text{Ca}^{2+} - \text{HCO}_3^-)$  and  $\text{SO}_4^{2-}$  were poor ([Figure 7E](#)). Furthermore, most samples were undersaturated in

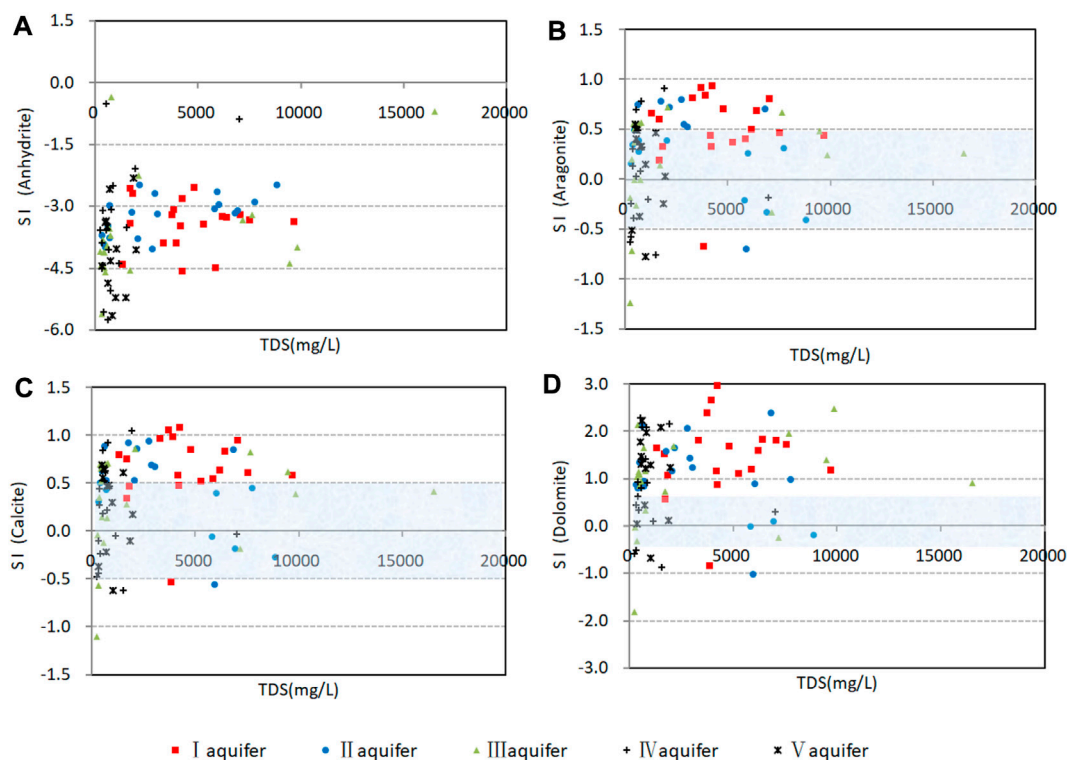


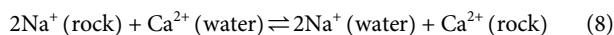
FIGURE 10

Saturation indices of confined groundwater in the study area. (A) Saturation indices values for anhydrite. (B) Saturation indices values for aragonite. (C) Saturation indices values for calcite. (D) Saturation indices values for dolomite.

gypsum ( $SI < -2$ ; Figure 10A). Confined aquifers in the study area have excellent sealing properties, low mobility, and long retention times, so evaporite deposits such as gypsum are at low levels and  $SO_4^{2-}$  is mainly derived from insoluble sulfides (Lang et al., 2011), although the high  $SO_4^{2-}$  contents of some samples are attributable to anthropogenic activity.

### 3.5 Cation exchange

In terms of hydrochemical processes and ion sources,  $Ca^{2+}$ ,  $Mg^{2+}$ , and  $Na^+$  deviated slightly from the standard model, which implied that the groundwater was affected by other factors. Cation exchange commonly influences the evolution of groundwater composition (Tourmassat et al., 2009; Zheng et al., 2021) through typical reactions as follows:



The reactions on the right are positive cation exchange, and those to the left are reverse cation exchange. The relationship between  $(Mg^{2+} + Ca^{2+} - HCO_3^- - SO_4^{2-})$  and  $(Na^+ + K^+ - Cl^-)$  indicates the mechanism of cation exchange (Figure 8).

Changes in  $(Mg^{2+} + Ca^{2+} - HCO_3^- - SO_4^{2-})$  and  $(Na^+ + K^+ - Cl^-)$  for the samples were opposite with a correlation coefficient of 0.98, which indicated a strong negative correlation. In general, the anion changes ( $Cl^-$ ,  $HCO_3^-$ ,  $SO_4^{2-}$ ) in the groundwater were not significant, so this negative correlation mainly reflects  $(Ca^{2+}$ ,

$Mg^{2+})$  and  $(Na^+, K^+)$ . A clear relationship between  $(Ca^{2+}, Mg^{2+})$  and  $(Na^+, K^+)$  is thus noted with cation exchange playing a major role in controlling the hydrochemical compositions of groundwater.

The direction of cation exchange depends on the ionic adsorption energy and concentration. The energy decreases in the order of  $Ca^{2+} > Mg^{2+} > K^+ > Na^+$ , so positive cation exchange is more common and leads to an increase in  $Na^+$  and  $K^+$  and a decrease in  $Ca^{2+}$  and  $Mg^{2+}$  concentrations in groundwater. However, 61% of the samples in the study area exhibited reverse cation exchange with negative  $(Na^+ + K^+ - Cl^-)$  and positive  $(Mg^{2+} + Ca^{2+} - HCO_3^- - SO_4^{2-})$  values.

Reverse cation exchange is more common in water with  $Cl^-$  content of  $>7.5 \text{ meq L}^{-1}$  (Figures 8C, D), whereas positive cation exchange is predominant with  $Cl^- < 7.5 \text{ meq L}^{-1}$ . This is consistent with the demarcation index for groundwater origins (Section 3.4). Reverse cation exchange is more significant in marine–continental-origin groundwater, and positive cation exchange is more significant in continental-origin groundwater with cation exchange explaining the deviation of some samples from the Gibbs model and why the  $Na^+/Cl^-$  ratio is below the 0.87:1 line.

### 3.6 Anthropogenic activity and hydrochemical evolution

As a drainage area of the Yangtze River Delta, aquifers in the study area have received freshwater recharge throughout geological history through lateral inflow, which compresses saline water within

a certain range and limits its expansion and forms stable boundaries. However, boundaries and hydrochemical characteristics have changed over the past century due to groundwater exploitation.

Annual groundwater use exceeded 200 million m<sup>3</sup> in 1963, but it is currently decreasing each year. During the heavy-use periods, groundwater funnels develop due to excessive use, and saline water flows into the fresh water. Thus, continental-origin groundwater becomes marine–continental-origin groundwater (Figure 9). For example, saline water from the east flowed into a groundwater funnel to the northwest of Qingpu in aquifer III.

The expansion of saline water due to human activities over the past century is widespread and has serious implications for freshwater resources. Fortunately, Shanghai has adopted strict controls on groundwater exploitation with annual use limited to 2 million m<sup>3</sup>. Artificial recharge has also been implemented. During the 13th Five Year Plan period, the annual artificial recharge was ~20 million m<sup>3</sup> and through this the groundwater level rises each year. However, artificial recharge has caused other problems, notably, desalination and mineral re-dissolution.

Saturation indices were calculated with respect to gypsum, aragonite, calcite, and dolomite in groundwater and are plotted in Figure 10. It is generally considered that groundwater is saturated at SI values of -0.5 to +0.5 (Liu, 2019). Most samples were supersaturated or saturated in aragonite, calcite, and dolomite (SI >-0.5; Figures 10B–D), which is consistent with weak hydrodynamic conditions in the study area. However, a few samples had SI values of <-0.5, which is possibly because of the influx of fresh groundwater and artificial recharge and resulted in the breakdown of hydrochemical equilibrium and renewed mineral dissolution (Kanagaraj and Elango, 2019).

## 4 Conclusion

The hydrochemical characteristics of groundwater were studied and trends in the study area were identified. These findings are valuable for planning groundwater protection and utilization in Shanghai.

Hydrochemical characteristics are dominated by the origin of groundwater. Two groundwater origins were identified: marine–continental- and continental-origin. For marine–continental-origin groundwater, major ions are primarily derived from ancient seawater and carbonate dissolution, and reverse cation exchange is common due to high concentrations of Na. Silicate weathering, carbonate dissolution, and positive cation exchange predominantly contribute to the hydrochemical composition of continental-origin groundwater.

TDS contents of 1,000 mg L<sup>-1</sup> and hydrochemical facies do not accurately identify the origins of groundwater, but Cl<sup>-</sup> content of

7.5 meq L<sup>-1</sup> acts as a demarcation index for the two origins. This index can be used to determine the boundaries between the groundwater of the two origins and allows accurate monitoring and prediction of the advance/retreat of saline water.

We mainly focused on the relationship between groundwater and human activities, which is unavoidable in Shanghai. The study demonstrates that geogenic processes are not the only mechanisms controlling groundwater chemistry; anthropogenic activities also affect groundwater chemistry, and once the evolution of groundwater is disturbed, then recovery is difficult.

## Data availability statement

The original contributions presented in this study are included in the article/Supplementary Material, and further inquiries can be directed to the corresponding author.

## Author contributions

All authors listed have made a substantial, direct, and intellectual contribution to the work and approved it for publication.

## Funding

This research was supported by a special project on Asian cooperation (Comparative study of geo-environment and geohazards in the Yangtze River Delta and Red River Delta) and a study of three-dimensional geological models and environmental physical fields of middle–shallow underground space.

## Conflict of interest

The authors declare that the research was conducted in the absence of any commercial or financial relationships that could be construed as a potential conflict of interest.

## Publisher's note

All claims expressed in this article are solely those of the authors and do not necessarily represent those of their affiliated organizations, or those of the publisher, the editors, and the reviewers. Any product that may be evaluated in this article, or claim that may be made by its manufacturer, is not guaranteed or endorsed by the publisher.

## References

- An, T. D., Tsujimura, M., Phu, V. L., Kawachi, A., and Ha, D. T. (2014). Chemical characteristics of surface water and groundwater in coastal watershed, mekong delta, vietnam. *Environ. Sci.* 20, 10. doi:10.1016/j.proenv.2014.03.085
- Bau, M., Alexander, B., Chesley, J. T., Dulski, P., and Brantley, S. L. (2004). Mineral dissolution in the cape cod aquifer, Massachusetts, USA: I. Reaction stoichiometry and impact of accessory feldspar and glauconite on strontium isotopes, solute concentrations, and REY distribution. *Geochimica Cosmochimica Acta* 68 (6), 1199–1216. doi:10.1016/j.gca.2003.08.015
- Farid, I., Zouari, K., Rigane, A., and Beji, R. (2015). Origin of the groundwater salinity and geochemical processes in detrital and carbonate aquifers: Case of chougafiya basin (central Tunisia). *J. Hydrology* 530, 508–532. doi:10.1016/j.jhydrol.2015.10.009

- Gibbs, R. J. (1970). Mechanisms controlling world water chemistry. *Science* 170 (3962), 1088–1090. doi:10.1126/science.170.3962.1088
- Gibbs, R. J. (1972). Water chemistry of the amazon river. *Geochimica Cosmochimica Acta* 36 (9), 1061–1066. doi:10.1016/0016-7037(72)90021-x
- Gan, Y., Zhao, K., Deng, Y., Liang, X., Ma, T., and Wang, Y. (2018). Groundwater flow and hydrogeochemical evolution in the jiangnan plain, central China. *Hydrogeology J.* 26 (5), 1609–1623. doi:10.1007/s10040-018-1778-2
- Gianguzza, A., Milea, D., Millero, F. J., and Sammartano, S. (2004). Hydrolysis and chemical speciation of dioxouranium(vi) ion in aqueous media simulating the major ion composition of seawater. *Mar. Chem.* 85 (3–4), 103–124. doi:10.1016/j.marchem.2003.10.002
- Gong, S. L. (2009). Change of groundwater seepage field and its influence on the development of land subsidence in shanghai. *Scispace* 20 (3), 1–5. doi:10.3969/j.issn.1007-1903.2009.01.001
- Gu, X., Xiao, Y., Yin, S., Hao, Q., Liu, H., Hao, Z., et al. (2018). Hydrogeochemical characterization and quality assessment of groundwater in a long-term reclaimed water irrigation area, north China plain. *Water* 10 (9), 1209. doi:10.3390/w10091209
- Huang, S., Yin, Y., Sun, R., and Tan, X. (2021). *In situ* anaerobic bioremediation of petroleum hydrocarbons in groundwater of typical contaminated site in shanghai, China: A pilot study. *Environ. Eng. Sci.* 38, 1052–1064. doi:10.1089/ees.2020.0534
- Jang, C. S., Liu, C. W., and Chou, Y. L. (2012). Assessment of groundwater emergency utilization in taipei basin during drought. *J. Hydrology* 414, 405–412. doi:10.1016/j.jhydrol.2011.11.016
- Kanagaraj, G., and Elango, L. (2019). Chromium and fluoride contamination in groundwater around leather tanning industries in southern India: Implications from stable isotopic ratio  $\delta^{53}\text{Cr}/\delta^{52}\text{Cr}$ , geochemical and geostatistical modelling. *Chemosphere* 220, 943–953. doi:10.1016/j.chemosphere.2018.12.105
- Kenoyer, G. J., and Bowser, C. J. (1992). Groundwater chemical evolution in a sandy silicate aquifer in northern Wisconsin: 1. Patterns and rates of change. *Water Resour. Res.* 28 (2), 579–589. doi:10.1029/91WR02302
- Kim, K. (2010). Plagioclase weathering in the groundwater system of a sandy, silicate aquifer. *Hydrol. Process.* 16 (9), 1793–1806. doi:10.1002/hyp.1081
- Kunwar, B., and Kawamura, K. (2014). One-year observations of carbonaceous and nitrogenous components and major ions in the aerosols from subtropical okinawa island, an outflow region of Asian dusts. *Atmos. Chem. Phys.* 14 (4), 1819–1836. doi:10.5194/acpd-13-22059-2013
- Lang, Y. C., Liu, C. Q., Li, S. L., Zhao, Z. Q., and Zhou, Z. H. (2011). Tracing natural and anthropogenic sources of dissolved sulfate in a karst region by using major ion chemistry and stable sulfur isotopes. *Appl. Geochem.* 26, S202–S205. doi:10.1016/j.apgeochem.2011.03.104
- Li, C., Men, B.-H., and Yin, S.-Y. (2022). Analysis of groundwater chemical characteristics and spatiotemporal evolution trends of influencing factors in southern beijing plain. *Front. Environ. Sci.* 10, 913542. doi:10.3389/feenvs.2022.913542
- Li, M. G., Chen, J. J., Xu, Y. S., Tong, D. G., and Shi, Y. J. (2021). Effects of groundwater exploitation and recharge on land subsidence and infrastructure settlement patterns in shanghai. *Eng. Geol.* 282, 105995. doi:10.1016/j.enggeo.2021.105995
- Liu, C. W., and Wu, M. Z. (2019). Geochemical, mineralogical and statistical characteristics of arsenic in groundwater of the lanyang plain, taiwan. *J. Hydrology* 577, 123975. doi:10.1016/j.jhydrol.2019.123975
- Panno, S. V., Hackley, K. C., Hwang, H. H., Greenberg, S., Krapp, I., Landsberger, S., et al. (2006). Characterization and identification of na-cl sources in ground water. *Ground water* 44 (2), 176–187. doi:10.1111/j.1745-6584.2005.00127.x
- Qiu, J. B., and Li, X. (2007). *Quaternary Strata and sedimentary Environment in Shanghai*. Shanghai Chian: Shanghai Scientific and Technical Publishers.
- Rezaei, M., Sanz, E., Raeisi, E., Ayora, C., Vazquez-Suné, E., and Carrera, J. (2005). Reactive transport modeling of calcite dissolution in the fresh-salt water mixing zone. *J. Hydrology* 311 (1–4), 282–298. doi:10.1016/j.jhydrol.2004.12.017
- Tournassat, C., Gailhanou, H., Crouzet, C., Braibant, G., Gautier, A., and Gaucher, E. C. (2009). Cation exchange selectivity coefficient values on smectite and mixed-layer illite/smectite minerals. *Soil Sci. Soc. Am. J.* 73 (3), 928–942. doi:10.2136/sssaj2008.0285
- Wang, S., Xie, Z., Wang, F., Zhang, Y., Wang, W., Liu, K., et al. (2022). Geochemical characteristics and quality appraisal of groundwater from Huatugou of the Qaidam Basin on the Tibetan plateau. *Front. Earth Sci.* 10, 874881. doi:10.3389/feart.2022.874881
- Wei, Z. X., Zai, G. Y., and Yan, X. X. (2010). *Atlas of Shanghai urban Geology*. China: Geological Publishing House.
- Yang, N., Wang, G., Shi, Z., Zhao, D., Jiang, W., Guo, L., et al. (2018). Application of multiple approaches to investigate the hydrochemistry evolution of groundwater in an arid region: Nomhon, northwestern China. *Water* 10 (11), 1667. doi:10.3390/w10111667
- Zhang, X., Hui, Q., Wu, H., Chen, J., and Qiao, L. (2016). Multivariate analysis of confined groundwater hydrochemistry of a long-exploited sedimentary basin in northwest China. *J. Chem.* 2016, 1–15. doi:10.1155/2016/3812125
- Zhang, W., Qin, X., and Yi, L. (1999). Groundwater system and ITS characteristics in Shanghai region. *Carsologica Sin.* 1999(4), 343–351. doi:10.3969/j.issn.1001-4810.1999.04.007
- Zheng, Z., Gla, B., Xs, B., Xz, B., Lei, W. B., Fu, H., et al. (2021). Geochemical controls on the enrichment of fluoride in the mine water of the shendong mining area, China. *Chemosphere* 284, 131388. doi:10.1016/j.chemosphere.2021.131388